NOTES AND CORRESPONDENCE

Comments on "The Diagnosis of Synoptic-Scale Vertical Motion in an Operational Environment"

CHUNG-CHIENG LAI

Department of Atmospheric Science, State University of New York at Albany, Albany, New York

15 January 1988 and 1 August 1988

It was a pleasure to read the paper by Durran and Snellman (1987, hereafter referred to as DS) on various techniques for calculating the forcing terms of the quasi-geostrophic omega equation. Several flaws found in DS have prompted the author to perform additional calculations and to modify the explanation for the error incurred in calculating individual terms in the quasi-geostrophic omega equation.

Barnes (1986) discusses the accuracy of algorithms used to compute the forcing term of the omega equation. However, the discussion is limited to the Q-vector approach (Hoskins et al. 1978). The three techniques cited in DS for computing the total forcing of the omega equation are 1) the traditional approach, 2) Trenberth's (1978) approach, and 3) Hoskins' approach. If the β-effect[1] is neglected, the total forcing (TF) obtained through these three approaches is equivalent analytically and can be expressed as (in conventional symbols)

- Traditional approach:

$$\mathrm{TF} = f_0 \frac{\partial}{\partial p}\left[\mathbf{V}_g \cdot \nabla\left(\frac{1}{f_0} \nabla^2 \phi + f \right) \right] + \nabla^2\left[\mathbf{V}_g \cdot \nabla\left(-\frac{\partial \phi}{\partial p} \right) \right].$$

- Trenberth's approach:

$$\mathrm{TF} = f_0 \frac{\partial \mathbf{V}_g}{\partial p} \cdot \nabla\left(\frac{1}{f_0} \nabla^2 \phi + f \right) + f_0 \mathbf{V}_g \cdot \nabla\left(\frac{1}{f_0} \frac{\partial}{\partial p} \nabla^2 \phi \right) + \frac{\partial \mathbf{V}_g}{\partial p} \cdot \nabla(\nabla^2 \phi) - \mathbf{V}_g \cdot \nabla\left(\frac{\partial}{\partial p} \nabla^2 \phi \right) - 2\left[\mathbf{J}\left(v_g, \frac{\partial v_g}{\partial p} \right) + \mathbf{J}\left(u_g, \frac{\partial u_g}{\partial p} \right) \right]$$

$$= 2 \frac{\partial \mathbf{V}_g}{\partial p} \cdot \nabla(\nabla^2 \phi) - 2\left[\mathbf{J}\left(v_g, \frac{\partial v_g}{\partial p} \right) + \mathbf{J}\left(u_g, \frac{\partial u_g}{\partial p} \right) \right],$$

$\mathbf{J}$ is the Jacobian.

- Hoskins' approach:

$$\mathrm{TF} = -2\left[\frac{\partial}{\partial x}\left(\frac{\partial \mathbf{V}_g}{\partial x} \cdot \nabla\left(\frac{\partial \phi}{\partial p} \right) \right) + \frac{\partial}{\partial y}\left(\frac{\partial \mathbf{V}_g}{\partial y} \cdot \nabla\left(\frac{\partial \phi}{\partial p} \right) \right) \right].$$

However, the values of the total forcing obtained through these three approaches may *not* be the same when calculated numerically with a finite difference approximation.

For simplicity, all of the computations of individual or combined forcing terms are performed on a Cartesian grid with a mesh size of 50 km × 50 km. The Coriolis parameter has the value at 46.6°N (the mean latitude of the domain of Fig. 12 of DS). The vertical levels used in the calculation are the same as used in DS.

Durran and Snellman have shown that when the vertical resolution is increased from 200 mb to 50 mb, the difference between the total forcing evaluated through the traditional approach and Hoskins' approach decreases. They also indicate that the largest errors occur in regions where $-\mathbf{V}_g \cdot \nabla\left(\frac{\partial}{\partial p} \nabla^2 \phi \right)$ is strongest. However, it will be shown here that the largest errors occur in the regions where the vertical shear of advection of thermal vorticity by the thermal wind (ATVTW) is strongest. The configuration of the height field and temperature field of DS's choice[2] (hereafter referred to as case A, see Fig. 1a), accidentally sets the region where $-\mathbf{V}_g \cdot \nabla\left(\frac{\partial}{\partial p} \nabla^2 \phi \right)$ is strongest close to

[1] The β-effect takes slightly different forms in the traditional approach and Hoskins' approach. The term $(\beta f_0 / f)(\partial^2 \phi / \partial p \partial x)$ in the traditional approach is replaced by a term $(2\beta^2 g / f^3)(\partial^3 \phi / \partial p \partial x \partial y)$ in Hoskins' approach.

[2] The set of analytic functions given in appendix C of DS appears to be erroneous. Durran and Snellman have sent a corrigendum to the editors.

Corresponding author address: Dr. Chung-Chieng Lai, State University of New York at Albany, Albany, NY 12222.

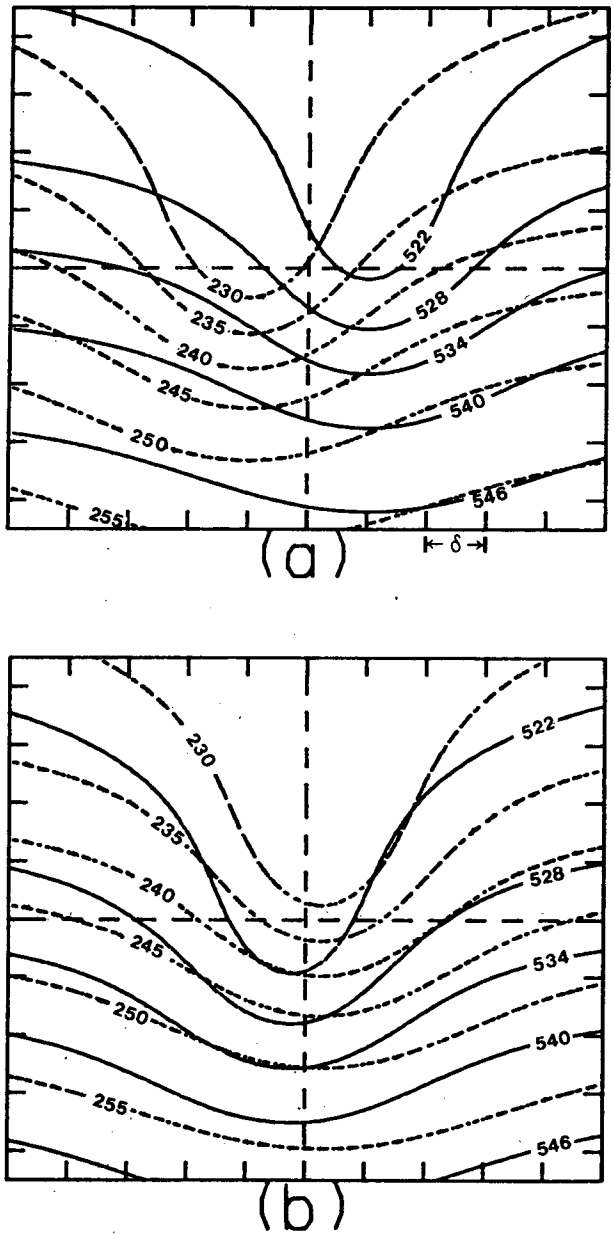

FIG. 1. (a) Contours of 500 mb height (solid, 6 dam contour interval) and temperature (broken, 5 K contour interval) according to DS's functions in Cartesian coordinates (case A). The distance between two tick marks, δ, is 200 km. (b) As in (a) except according to (1) and (2) (case B).

where the vertical shear of advection of thermal vorticity by the thermal wind is strongest.

One can see from Fig. 2 that in case A the two extremes of $-\frac{\partial \mathbf{V}_g}{\partial p}\cdot\nabla(\nabla^2\phi)$ flank the trough line of 500 mb height field, while the two extremes of $-\mathbf{V}_g\cdot\nabla\left(\frac{\partial}{\partial p}\nabla^2\phi\right)$ flank the 500 mb thermal trough. Trenberth's total forcing and Hoskins' total forcing both have the same pattern as that of $-\frac{\partial \mathbf{V}_g}{\partial p}\cdot\nabla(\nabla^2\phi)$. Their difference (not shown) is less than 1% and is caused by the horizontal resolution. On the other hand, the pattern of traditional total forcing is substantially different from that of Hoskins' total forcing. Their difference (DIFF) shows a pair of elongated ovals flanking the 500 mb thermal trough. (Note the contour interval for panel *f* is different from that of other panels.) If we carefully compare the patterns of $-\mathbf{V}_g\cdot\nabla\left(\frac{\partial}{\partial p}\nabla^2\phi\right)$ and DIFF we find that the major axis of the oval pattern of $-\mathbf{V}_g\cdot\nabla\left(\frac{\partial}{\partial p}\nabla^2\phi\right)$ does not align with that of DIFF. This implies that the largest error incurred in the computation of the total forcing using the traditional approach does not necessarily occur in the regions where $-\mathbf{V}_g\cdot\nabla\left(\frac{\partial}{\partial p}\nabla^2\phi\right)$ is strongest.

The following case (hereafter referred to as case B, see Fig. 1b) serves to prove that the DIFF is independent of $-\mathbf{V}_g\cdot\nabla\left(\frac{\partial}{\partial p}\nabla^2\phi\right)$. In case B, the gradients and the patterns of 500 mb height field and temperature field are kept the same as in case A. Only the locations of the 500 mb geopotential trough line and the thermal trough line are rearranged. The trough line of height field is to the southwest of the trough line of temperature field. The set of functions for case B is

$$h(x, y, 500) = 5370 - 143\tan^{-1}\left[\frac{\pi(y - y_c + y_1)}{2\,000\,000}\right] - 160\left[\left(\frac{x - x_c + x_1}{400\,000}\right)^2 + \left(\frac{y - y_c + y_1}{500\,000}\right)^2 + 1\right]^{-1}, \quad (1)$$

$$T(x, y, 500) = 245 - 14.3\tan^{-1}\left[\frac{\pi(y - y_c - y_1)}{2\,000\,000}\right] - 18\left[\left(\frac{x - x_c - x_1}{400\,000}\right)^2 + \left(\frac{y - y_c - y_1}{500\,000}\right)^2 + 1\right]^{-1}, \quad (2)$$

where $x_1 = 50\,000$, and $y_1 = 150\,000$.

Figure 3 has the same format as that of Fig. 2, except that it is for case B. Compared to Figs. 2b and 2d, Figs. 3b and 3d show a weaker field of $-\mathbf{V}_g\cdot\nabla\left(\frac{\partial}{\partial p}\nabla^2\phi\right)$, and a stronger field of traditional total forcing. All other fields in case B are competitive with their counterpart in case A. The (minimum) center of $-\mathbf{V}_g\cdot\nabla\left(\frac{\partial}{\partial p}\nabla^2\phi\right)$ is located exactly between the two centers (minimum and maximum) of the difference

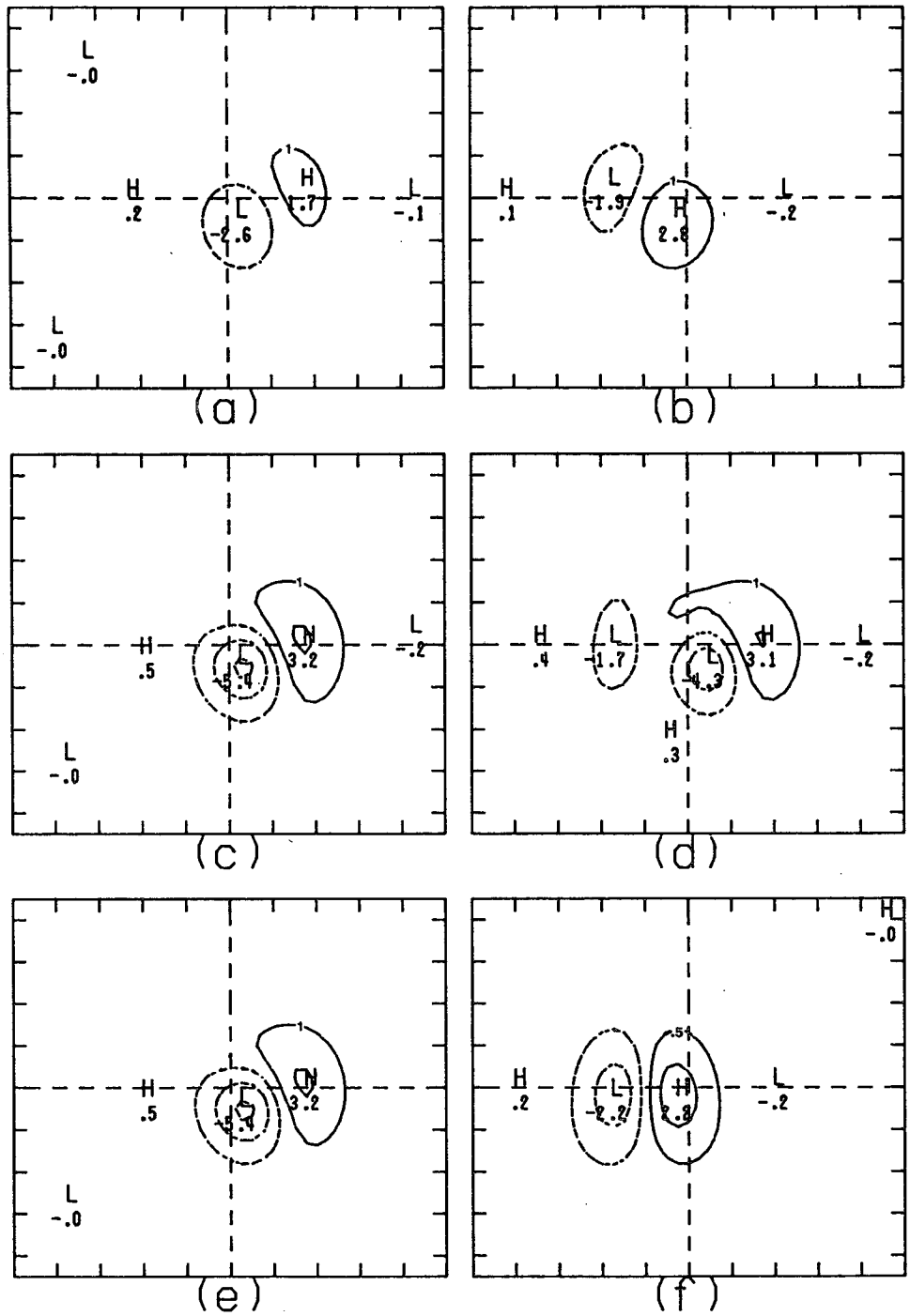

FIG. 2. Forcing terms of quasi-geostrophic omega equation for case A. Units: 10^{-16} m kg^{-1} s^{-1}. The H and L indicate maxima and minima, respectively. Solid (broken) lines are for positive (negative) values. (a) $-\frac{\partial \mathbf{V}_g}{\partial p}\cdot\nabla(\nabla^2\phi)$, (b) $-\mathbf{V}_g\cdot\nabla\left(\frac{\partial}{\partial p}\nabla^2\phi\right)$, (c) Trenberth's total forcing, (d) traditional total forcing, (e) Hoskins' total forcing, and (f) difference (DIFF) between traditional total forcing and Hoskins' total forcing. Contour interval is 2 for (a) through (e), 1 for (f). See text for explanation.

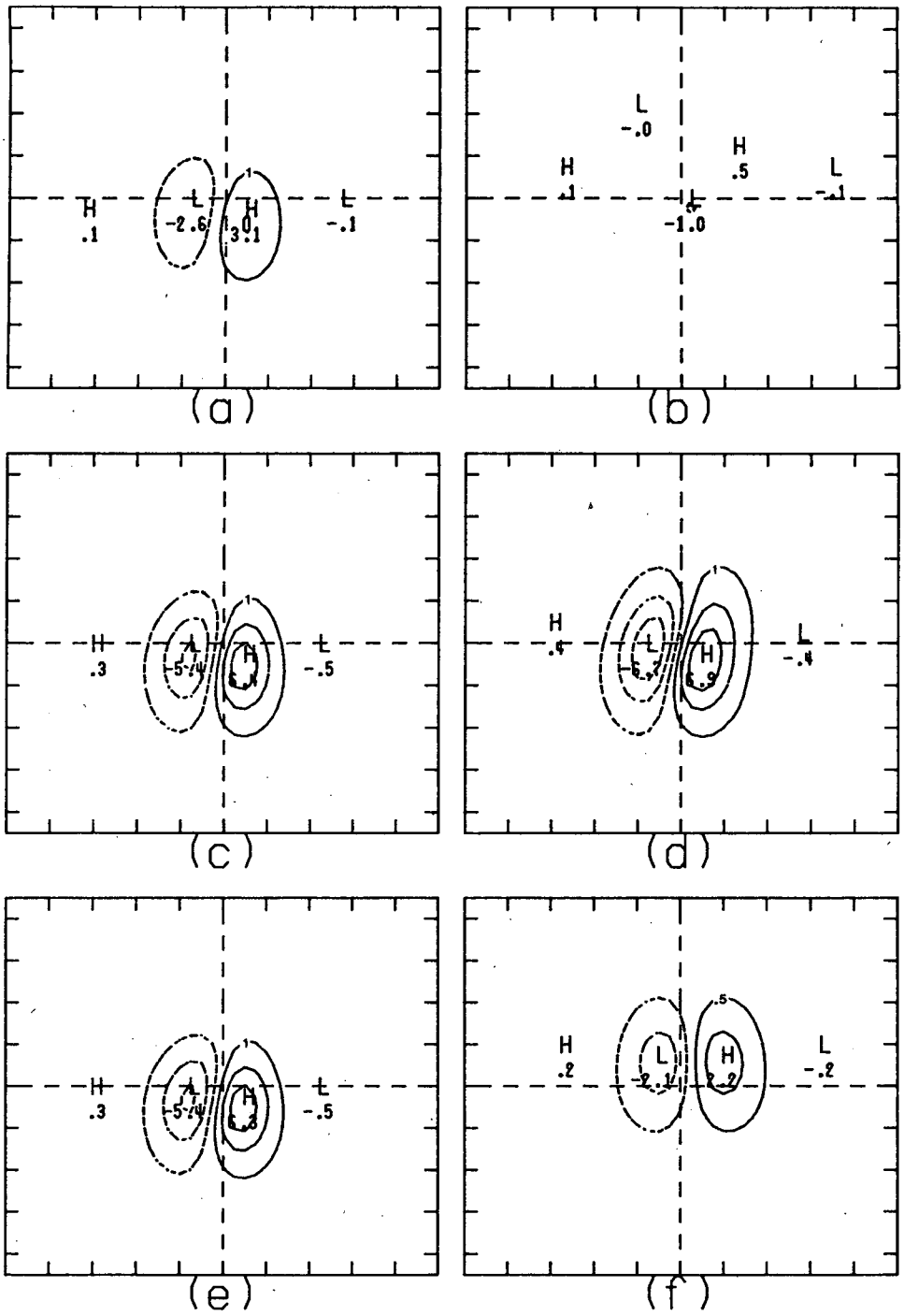

FIG. 3. As in Fig. 2, except for case B.

(DIFF) between the traditional total forcing and Hoskins' total forcing. It is now apparent that DIFF is independent of $-\mathbf{V}_g \cdot \nabla\left(\frac{\partial}{\partial p} \nabla^2 \phi\right)$.

What is the real cause of this error (DIFF)? Durran and Snellman argue that the numerical expression (B4) [of DS] does not decompose into the numerical expressions for $\frac{\partial \mathbf{V}_g}{\partial p} \cdot \nabla(\nabla^2 \phi)$ and $\mathbf{V}_g \cdot \nabla\left(\frac{\partial}{\partial p} \nabla^2 \phi\right)$, and the numerical expression (B5) does not decompose into the numerical expressions for $\frac{\partial \mathbf{V}_g}{\partial p} \cdot \nabla(\nabla^2 \phi)$,

$-\mathbf{V}_g\cdot\nabla\left(\frac{\partial}{\partial p}\nabla^2\phi\right)$ and $-2\left[\mathbf{J}\left(u_g, \frac{\partial u_g}{\partial p}\right) + \mathbf{J}\left(u_g, \frac{\partial v_g}{\partial p}\right)\right]$. Therefore, when (B4) and (B5) are added, $-\mathbf{V}_g\cdot\nabla\left(\frac{\partial}{\partial p}\nabla^2\phi\right)$ does not cancel exactly. This argument is not completely correct. Barnes (1986) indicates that, in the horizontal, finite-difference errors are acceptably small for waves with wavelengths longer than nine or more grid intervals. In fact, if the horizontal resolution is increased further, the finite difference approximation approaches the continuous value. So, the value of $\nabla^2\left[\mathbf{V}_g\cdot\nabla\left(-\frac{\partial\phi}{\partial p}\right)\right]$, expressed as (B5) in DS, is equal to the sum of $\frac{\partial\mathbf{V}_g}{\partial p}\cdot\nabla(\nabla^2\phi)$, $-\mathbf{V}_g\cdot\nabla\left(\frac{\partial}{\partial p}\nabla^2\phi\right)$ and $-2\left[\mathbf{J}\left(u_g, \frac{\partial u_g}{\partial p}\right) + \mathbf{J}\left(v_g, \frac{\partial v_g}{\partial p}\right)\right]$. However, the increase of horizontal resolution cannot make the value of $f_0\frac{\partial}{\partial p}\left[\mathbf{V}_g\cdot\nabla\left(\frac{1}{f_0}\nabla^2\phi\right)\right]$ obtained through (B4) equal to the sum of $\frac{\partial\mathbf{V}_g}{\partial p}\cdot\nabla(\nabla^2\phi)$ and $\mathbf{V}_g\cdot\nabla\left(\frac{\partial}{\partial p}\nabla^2\phi\right)$, since the problem comes from the product rule in the p-coordinate [see (B11) and (B12) of DS]. For simplicity, assume a differential form in the horizontal is being used. So, $\nabla^2\left[\mathbf{V}_g\cdot\nabla\left(-\frac{\partial\phi}{\partial p}\right)\right]$ gets the same values from the traditional approach and from Trenberth's approach. In addition, both Trenberth's total forcing and Hoskins' total forcing have exact values. What, then, does the difference (DIFF) between the traditional total forcing and Hoskins' total forcing represent? It represents the difference between the numerical expressions of the left-hand side (LHS) and right-hand side (RHS) of (B11) of DS. However, it can be further manipulated as follows:

$$\begin{aligned}\text{DIFF} &= \frac{A_{i+1}B_{i+1} - A_{i-1}B_{i-1}}{2\Delta} - \frac{A_i(B_{i+1} - B_{i-1}) + B_i(A_{i+1} - A_{i-1})}{2\Delta} \\ &= \frac{(A_{i+1} - A_i)(B_{i+1} - B_i) - (A_i - A_{i-1})(B_i - B_{i-1})}{2\Delta} \\ &= \frac{\Delta}{2}\frac{A_{i+1} - A_i}{\Delta}\frac{B_{i+1} - B_i}{\Delta} - \frac{\Delta}{2}\frac{A_i - A_{i-1}}{\Delta}\frac{B_i - B_{i-1}}{\Delta},\end{aligned} \tag{3}$$

where A and B represent the $\mathbf{V}_g$ and $\nabla\left(\frac{1}{f_0}\nabla^2\phi\right)$, respectively. The Δ is the vertical resolution. The first term and the second term on the RHS of (3) are proportional to the advection of thermal vorticity by the geostrophic thermal wind at the $(500 + \Delta/2)$ mb and $(500 - \Delta/2)$ mb levels, respectively. Therefore, their difference is proportional to the vertical shear of the advection of thermal vorticity by the geostrophic thermal wind over Δ. It is a function of the 500 mb temperature field only and is antisymmetric to the thermal trough line. This error of the forcing calculated with the traditional approach is an artifact mainly due to the finite difference approximation with a coarse resolution in the vertical.

Acknowledgments. The author is indebted to an outstanding anonymous reviewer who offered many suggestions for making this paper more understandable. Ms. Sally Marsh and Dr. Dan Keyser polished the wording. The research was partially supported by NSF Grant ATM8311106.

REFERENCES

Barnes, S. L., 1986: On the accuracy of omega diagnostic computations. *Mon. Wea. Rev.*, **114**, 1664–1680.

Durran, D. R., and L. W. Snellman, 1987: The diagnosis of synoptic-scale vertical motion in an operational environment. *Wea. Forecasting*, **2**, 17–31.

Hoskins, B. J., I. Draghici and H. C. Davies, 1978: A new look at the ω-equation. *Quart. J. Roy. Meteor. Soc.*, **104**, 31–38.

Trenberth, K. E., 1978: On the interpretation of the diagnostic quasi-geostrophic omega equation. *Mon. Wea. Rev.*, **106**, 131–137.